Investigation of Flow Restrictors for Rack Level Two-Phase Cooling under Nonuniform Heating

Serdar Ozguc, Qingyang Wang, Akshith Narayanan, Richard W. Bonner III
Accelsius, Austin, TX, USA
sozguc@accelsius.com

Abstract
Conventional air-cooled systems in data centers are failing to address the increasing power densities brought by high-performance computing. Pumped direct-to-chip two-phase cooling offers a potential solution to thermal challenges in next-generation data centers owing to the high heat transfer coefficients and heat capacities associated with flow boiling. However, there are technical challenges to address such as flow maldistribution caused by nonuniform heating in highly parallel two-phase loops. Flow restrictors can be implemented to suppress the maldistribution, however, there is a need to better understand the requirements and performance cost of their use. To this end, this work analyzes flow maldistribution and restrictors in a server-rack level two-phase loop with 34 sleds cooled in parallel. A numerical system-level model is developed which relies on an empirical correlation to capture the pressure drop response of the flow components in the server sleds. Pressure drop data are collected experimentally at various heat inputs and flow rates to calibrate the empirical correlation. The resulting model is used to evaluate flow maldistribution and pressure drop cost of various flow restrictors. In the absence of restrictors, maldistribution due to nonuniform heating causes dry-out in cold plates even though the overall flow rate is adequate to dissipate the total heat input. Orifice restrictors which have quadratic scaling of pressure drop and mass flow rate, suppress the maldistribution below an acceptable limit at the cost of additional pressure drop twice as much as that of the sled itself. Restrictors with high order mass flow rate-to-pressure drop scaling, such as flow regulators, can suppress the maldistribution with significantly smaller pressure drop penalty at the cost of design complexity.

Keywords
flow boiling, flow maldistribution, direct-to-chip cooling, data center cooling

1. Introduction

Power usage in data centers account for 1.8% of the overall electricity expenditure in the United States [1] and the cooling infrastructures make up 50% of the total energy consumption of the data centers [2]. Power consumption translates to high operational costs and carbon footprint which can be potentially reduced by implementing higher efficiency thermal management systems. Moreover, the increasing power densities in data centers to address the demand for high-performance computing is beginning to push the thermal limits of the currently adopted air cooled systems.

The conventional data center architecture relies on Computer Room Air Handler (CRAH) or Computer Room Air Conditioner (CRAC) units to cool the air for dissipating the heat generated in the servers. Air-cooled systems offer convenience and reliability, bolstered by their extensive track record. However, liquid-cooled solutions were shown to significantly reduce the overall power consumption relative to air-cooling [3] and can handle increased power densities due to higher convective heat transfer and heat capacity. Single-phase liquid-cooling with water-based coolants can achieve good thermal performance due to water's favorable thermal characteristics. However, a minor leak in a water-cooled system can cause a catastrophic electrical failure. Two-phase liquid-cooling circumvents this problem with dielectric refrigerants where high heat transfer performance is achieved through flow boiling. Heat fluxes on the order of 1 kW/cm^2 have been dissipated using two-phase cooling [4].

Pumped two-phase cooling has been studied extensively in the literature [5]. However, implementation and testing of two-phase cooling in data center applications is limited. The highly parallel architecture of liquid-cooling loops in server racks can suffer from flow maldistribution of coolant between heat generating components. This problem is more prominent in two-phase flows because of the difference of pressure drop between liquid and vapor flows. High heat loads on cold plates result in increased vapor generation, leading to a rise in pressure drop. This, in turn, diverts the coolant through the cold plates with lower heat loads.

Flow restrictors can be adopted upstream of boiling [6] to suppress maldistribution by increasing the liquid line pressure drop relative to the vapor line. However, careful design of restrictors is crucial to effectively mitigate maldistribution without inducing excessive pressure drops that would reduce the overall flow rate of the system. To this end, the work presented here implements a numerical model to analyze a two-phase loop for cooling a data center rack with a total of 34 server sleds connected in a parallel flow configuration. First, the model is calibrated using empirical pressure drop data collected from single server sled experiments under flow boiling. Second, flow maldistribution is analyzed with and without orifice-type inlet restrictors which have quadratic scaling of pressure drop and mass flow rate. Lastly, the pressure drop cost of restrictors is evaluated for designs with different pressure drop/flow rate scaling.

2. Methodology

Severity of flow maldistribution is dependent on hydrodynamic and thermal characteristics of the overall flow loop. Therefore, optimal restrictor design is specific to a system. Throughout this paper, a two-phase flow loop for a data center rack consisting of 34 server sleds with heat generating components is investigated. A flow diagram of the loop can be seen in Figure 1. The amount of heat dissipated from each sled is between 0-2 kW (0-68 kW total) and can vary among sleds. Refrigerant R-1233zd(E) is used as the two-phase coolant in the main loop. A reservoir tank provides a buffer for changes in vapor/liquid volume with heat loads to prevent flooding of the condenser or vapor suction by the pump. The centrifugal pump after the reservoir sustains coolant flow across the loop and overcomes the pressure drop. Pumped coolant enters the sleds as liquid, removes the generated heat, and leaves as a

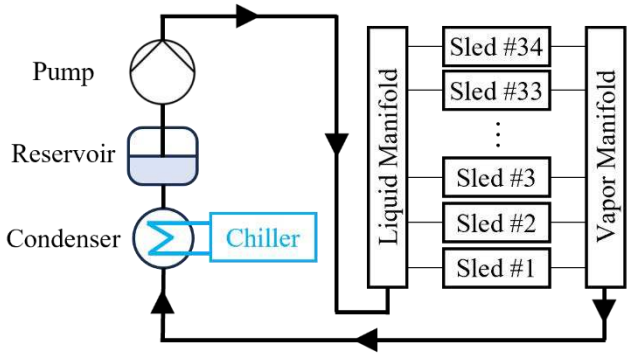

Figure 1. Flow diagram of the investigated server-rack level two-phase flow loop for data center cooling.

liquid/vapor mixture. The sleds are connected to the loop via a liquid manifold upstream and a vapor manifold downstream. The liquid and vapor manifolds are large pipes (1" and 2" inner diameter respectively) connected to sleds with additional tubing. A corrugated plate heat exchanger is used as the condenser wherein the liquid/vapor mixture dissipates the heat to a secondary water loop cooled by a chiller.

2.1. Maldistribution Model

The highly parallelized cooling architecture and potential nonuniform heating requires restrictors within each sled to prevent flow maldistribution. A numerical model of the liquid manifold, vapor manifold, and the server sleds is developed to analyze the maldistribution and design the appropriate restrictors. Two-phase flow is simplified using the homogenous flow assumption wherein the vapor bubbles and the surrounding liquid move at the same velocity. The liquid and vapor manifolds are discretized along the length using a staggered grid and the conservation equations for mass, momentum, and energy are derived. The advective terms are discretized using the first-order upwind scheme. Figure 2 shows a schematic drawing of a part of the mesh containing three sleds. The manifolds are connected by the server sleds in between. Additional conservation equations are derived for control volumes encapsulating individual sleds. The sleds are treated as black boxes with hydrodynamic and thermal responses determined empirically in Section 2.2. The resulting discretized conservation equations for the manifolds and the sleds are as follows.

$$\dot{m}_{in,i} = \dot{m}_{in,i+1} + \dot{m}_{sled,j} \quad [1]$$

$$\dot{m}_{out,i} = \dot{m}_{out,i+1} + \dot{m}_{sled,j} \quad [2]$$

$$\frac{\dot{m}_{in,i+1}^2 - \dot{m}_{in,i}^2}{\rho_f A_{in}^2} + \rho_f g \Delta H - \frac{dP_{pipe}}{dy}\Delta y = P_{in,j} - P_{in,j+1} \quad [3]$$

$$\left(\frac{\dot{m}_{out,i+1}^2}{\rho_{m,j} A_{out}^2} - \frac{\dot{m}_{out,i}^2}{\rho_{m,j-1} A_{out}^2}\right) + \rho_{m,j} g \Delta H + \frac{dP_{pipe}}{dy}\Delta y = P_{out,j-1} - P_{out,j} \quad [4]$$

$$\Delta P_{sled} + \Delta P_{restrictor} = P_{in,j} - P_{out,j} \quad [5]$$

$$\dot{m}_{out,i+1} x_{out,j+1} + \dot{m}_{sled,j} x_{sled,j} = \dot{m}_{out,i} x_{out,j} \quad [6]$$

$$\dot{m}_{sled,j} x_{sled,j} h_{fg} = Q_{in,j} \quad [7]$$

where $\dot{m}$, P, and x are mass flow rate, static pressure, and vapor quality. The subscripts *in*, *sled*, and *out* indicate liquid manifold, sled outlet, and vapor manifold variables respectively. A_{in} and A_{out} are the liquid and vapor manifold cross-sectional areas, g is the gravitational acceleration, Δy is the height difference between sleds, and Q_{in} is the heat input to a sled. The terms ΔP_{sled} and $\Delta P_{restrictor}$ are correlations for pressure drop across the server sled and the restrictor which are described in Sections 2.2 and 2.3.

Constant liquid density and viscosity (ρ_f, μ_f) are used whereas mixture density and viscosity (ρ_m, μ_m) are strongly dependent on the local vapor quality. The mixture density is calculated, and the mixture viscosity is estimated using the correlation by Cicchitti et al. [7] as follows.

$$\rho_m = \begin{cases} \dfrac{1}{\dfrac{1-x}{\rho_f} + \dfrac{x}{\rho_g}}, & 0 < x < 1 \\ \rho_g, & x \geq 1 \end{cases} \quad [8]$$

$$\mu_m = \begin{cases} \mu_f + x \cdot (\mu_g - \mu_f), & 0 < \chi < 1 \\ \mu_g, & x \geq 1 \end{cases} \quad [9]$$

where ρ_g and μ_g are the vapor density and viscosity respectively.

The frictional losses in the manifolds (dP_{pipe}/dy) are estimated using friction factor correlations for fully developed laminar [8] and turbulent flows [9] in circular channels as follows.

$$\frac{dP_{pipe}}{dy} = -f_D \frac{\rho}{2}\frac{u^2}{D} \quad [10]$$

$$f_D = \begin{cases} \dfrac{64}{Re}, Re \leq 2300 \\ \dfrac{1}{\left(0.8284 * log\left(\dfrac{10.31}{Re}\right)\right)^2}, 2300 < Re \end{cases} \quad [11]$$

where Re is the Reynolds number, f_D is the Darcy friction factor, u is the flow speed, and D is the pipe inner diameter.

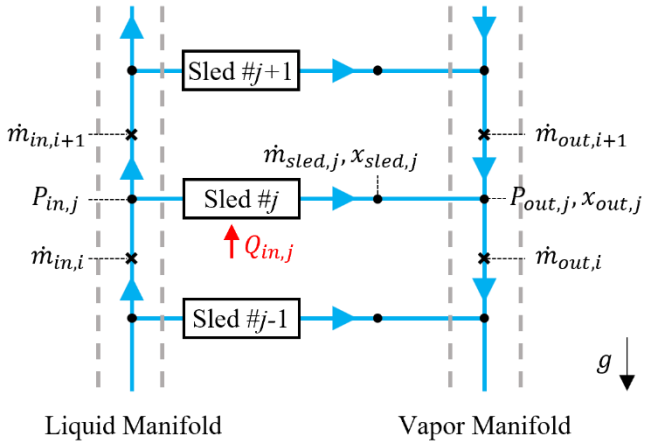

Figure 2. Schematic drawing of a part of the staggered mesh containing three sleds.

The two-phase loop is expected to dissipate up to 68 kW of heat maximum. A mass flow rate of 531 g/s is set as the inlet boundary condition to the liquid manifold which corresponds to an overall exit quality of 0.7 at the maximum heat input. The coolant enters as saturated liquid from the inlet. The properties of the refrigerant R-1233zd are evaluated at 40°C saturation temperature and are assumed constant. The resulting discretized conservation equations (Equations 1-7) are solved iteratively due to the nonlinearities.

2.2. Model Calibration

Two-phase pressure drop across a server sled (ΔP_{sled}) is difficult to estimate using physical equations due to the complex flow paths and geometries created by the bends, contractions, expansions, fittings, cold plates, etc. Instead, pressure drop of an individual sled is experimentally measured at various flow rates and heat inputs to derive an empirical correlation.

Flow diagram of the experimental flow loop can be seen in Figure 3. A test sled identical to the server sleds used in the rack-level cooling loop (Figure 1) is connected to a condenser, a reservoir, and a gear pump. The investigated server sled consists of two heat generating components which are emulated using two thermal test vehicles (TTV) with heat spreaders and cold plates. The two cold plates are connected in parallel and identical orifice plates are placed at the inlet of each to suppress instabilities. Ultrasonic flow meters are used to measure the flow rate across each TTV without interfering with the flow. Pressure drop across the sled with the orifice (ΔP_{total}) and the TTV (ΔP_{TTV}) are measured using differential pressure transducers. Four thermocouples embedded in each TTV heat spreader measure the temperature distribution. Additionally, coolant temperature is measured at the cold plate outlet using a probe thermocouple in the tubing.

Flow rate through the test sled is controlled using the gear pump. The TTVs are powered using an adjustable power supply to control the amount of heat input into the sled. The heat load of each TTV is equal. Pressure drop and temperature data are collected at various flow rates (5-26 g/s) and total heat inputs (0.2-2 kW) resulting in vapor qualities between 0-1. A total of 104 data points is collected. Throughout testing, saturation temperatures are kept between 30-50°C.

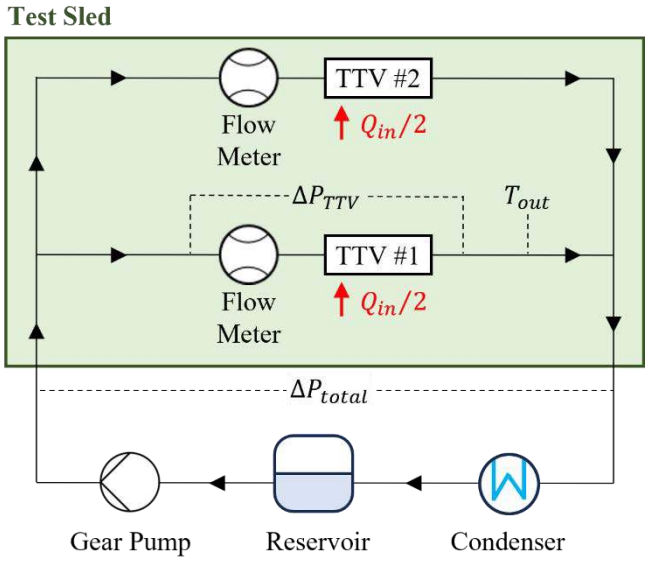

Figure 3. Flow diagram of the experimental flow loop for testing pressure drop across a server-sled.

The measured pressure drop across the sled (ΔP_{total}) contains the pressure drop due to the specific orifice used during calibration testing in addition to the sled components (ΔP_{sled}). The sled pressure drop is estimated from the total pressure drop as follows.

$$\Delta P_{sled} \approx \Delta P_{total} - \Delta P_{TTV,1P} \quad [12]$$

where $\Delta P_{TTV,1P}$ is the pressure drop across the TTV with the orifice under single-phase flow. Equation 12 assumes the single-phase pressure drop across the TTV is dominated by the orifice. A multi-variable second order polynomial fit is used to develop an empirical correlation for sled pressure drop (ΔP_{sled}) with respect to mass flow rate ($\dot{m}$) and exit vapor quality (x).

Thermal resistance of the sled is calculated using the measured temperatures and normalized as follows.

$$R = \frac{T_{HS.max} - T_{out}}{Q_{in}} \quad [13]$$

$$\bar{R} = \frac{R}{R_{ref}} \quad [14]$$

where R is the thermal resistance, $T_{HS,max}$ is the maximum temperature measured on the heat spreader surface for the two TTVs, Q_{in} is the total heat input, and R_{ref} is a reference thermal resistance used for normalizing. The boiling temperature is assumed to be equal to the measured coolant temperature at the TTV outlet (T_{out}) because the exit quality is kept between 0-1. Value of R_{ref} is set to the lowest thermal resistance value measured among the 104 data points collected.

2.3. Restrictor Model

Two restrictors are placed within each sled positioned upstream of the cold plates. The following equations are used for modeling pressure drop across restrictors.

$$\Delta\bar{P}_{restrictor} = \alpha\bar{m}^{\beta} \quad [15]$$

$$\bar{m} = \frac{\dot{m}_{sled}}{\dot{m}_{sled,ref}} \quad [16]$$

$$\Delta\bar{P}_{restrictor} = \frac{\Delta P_{restrictor}}{\Delta P_{sled,ref}} \quad [17]$$

where $\dot{m}_{sled,ref}$ and $\Delta P_{sled,ref}$ are the mass flow rate and pressure drop across an individual sled under flow boiling at maximum power, in the absence of flow maldistribution. Value of $\dot{m}_{sled,ref}$ is calculated from the overall flow rate input to the model whereas $\Delta P_{sled,ref}$ is a measured value during flow calibration experiments described in Section 2.2. Term α is the flow resistance factor and β is the flow scaling exponent. Based on the pressure drop normalization used in Equation 15, α represents the ratio of additional pressure drop introduced by the restrictor to the sled pressure drop at a flow rate of $\dot{m}_{sled,ref}$.

Values of α and β are dictated by the geometry of the restrictor and coolant properties. Linear scaling (β = 1) can be attained through a long tube with a small diameter where

viscous shear dominates the pressure drop. For orifice restrictors, pressure drop scales quadratically with mass flow rate (β = 2) due to a momentum dominated flow whereas the value of α depends on the orifice size. Higher order scaling can be achieved through moving or flexible parts in the restrictors. For example, commercial flow regulators incorporate flexible polymers that constrict the flow area with increasing pressure differential. Therefore, any increase in flow rate above the intended operating point results in a high pressure drop penalty. An ideal flow regulator provides an infinite scaling ($\beta \rightarrow \infty$) to deter flow maldistribution. However, α should be optimized through geometric design to avoid significant pressure drop when the flow rate is at the desired level. Flow maldistribution and pressure drop are investigated for various types of restrictors to assess their applicability in the two-phase flow loop.

3. Result

The test sled from Figure 3 is tested under various flow rates and exit vapor qualities. Resulting thermal resistance and pressure drops are recorded. Thermal resistance is strongly dependent on the exit vapor quality. Figure 4 shows thermal resistance at exit vapor qualities between 0-1 for all flow rates combined. The thermal resistance is lowest at 0.54 vapor quality and sharply increases near 0 and 1 as expected. The thermal performance improves from single-phase liquid cooling to higher vapor qualities as flow boiling provides enhanced convection and heat capacity. However, thermal resistance increases near $x_{sled} = 1$ because the generated vapor starts interfering with heat transfer. The two-phase loop shown in Figure 1 is designed to operate at an exit vapor quality of 0.7, however, individual sleds are expected to have higher qualities due to flow maldistribution. An upper limit of $x_{sled} = 0.85$ is chosen to ensure acceptable cooling performance in the sleds. Therefore, the objective in examining restrictor designs is to maintain a sufficiently low maldistribution to attain vapor qualities below 0.85.

Multi-variable, second-order polynomial fit is used for generating an empirical correlation from the experimentally collected pressure drop data. The resulting equation below correlates normalized sled pressure drop to normalized mass flow rate and exit vapor quality.

$$\Delta\bar{P}_{sled} = \frac{\Delta P_{sled}}{\Delta P_{sled,ref}} = 0.03\bar{m}^2 - 0.61x_{sled}^2 + 0.87\bar{m}x_{sled} + 0.05\bar{m} + -0.15x_{sled} - 0.24 \quad [18]$$

The developed correlation is used to predict the measured pressure drop. Predicted vs measured values can be seen in Figure 5. The correlation matches closely to the measured two-phase pressure drop with most of the predictions having less than 25% error. The numerical model summarized in Section 2.1 is updated with the empirical pressure drop correlation for flow maldistribution analysis.

The two-phase flow loop is analyzed without flow restrictors to serve as a benchmark. Uniform total heat input of 68 kW (2 kW per sled) is used. Figure 6.a shows the resulting exit vapor qualities for each sled. The flow is not uniform which results in an uneven exit vapor quality distribution under uniform heating because of gravitational effects. The liquid manifold is filled with liquid whereas the vapor manifold has a liquid/vapor mixture. The density difference between the liquid and mixture causes the sleds near the bottom to have a higher pressure difference and therefore a higher mass flow rate is achieved relative to the sleds near the top. Under uniform heating, exit vapor quality is lower for the sleds with higher flow rate. The lowest exit quality is 0.54 at the bottom sled whereas the highest exit quality is 0.88 at the top. The maximum vapor quality limit of 0.85 is not satisfied even under uniform heating when inlet restrictors are not used.

The maldistribution is expected to be higher than predicted; other flow boiling instabilities that might persist without flow restrictors are not accounted for by the numerical model. Instead, the focus is on the effect of nonuniform heating. In a server rack at a data center, the sleds might operate at different

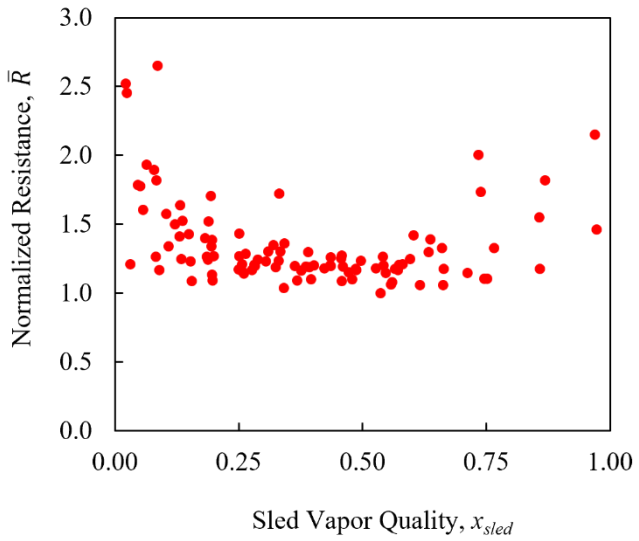

Figure 4. Experimental thermal resistance vs exit vapor quality for all flow rates tested.

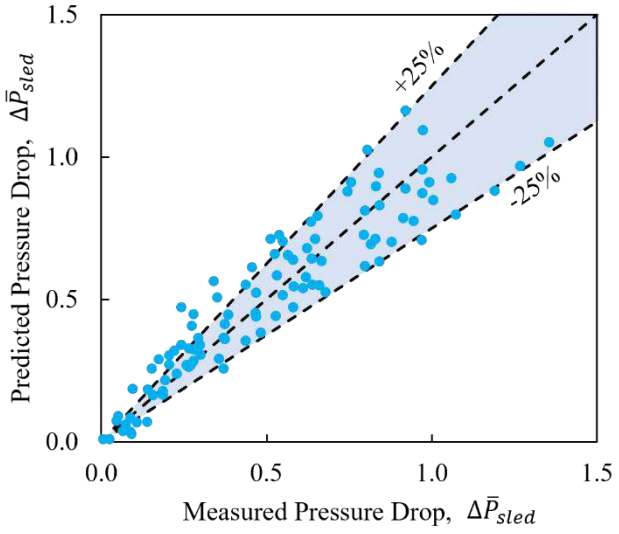

Figure 5. Predicted pressure drop vs experimentally measured pressure drop for all flow rates and heat inputs.

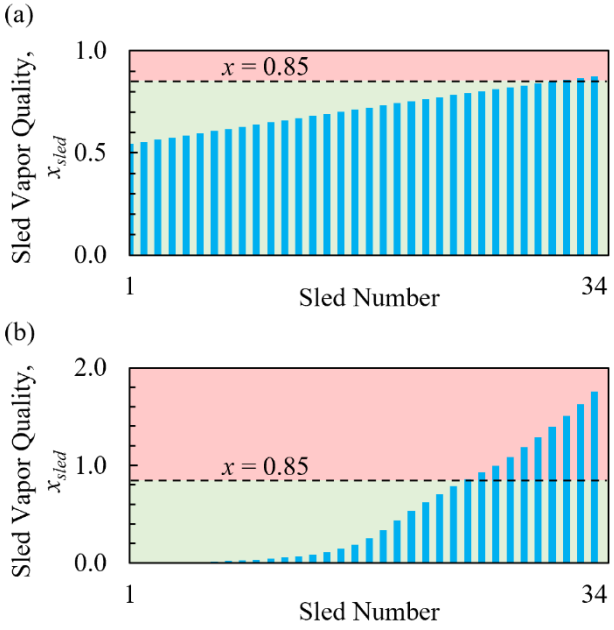

Figure 6. Predicted exit vapor quality distribution under (a) uniform and (b) nonuniform heating without flow restrictors.

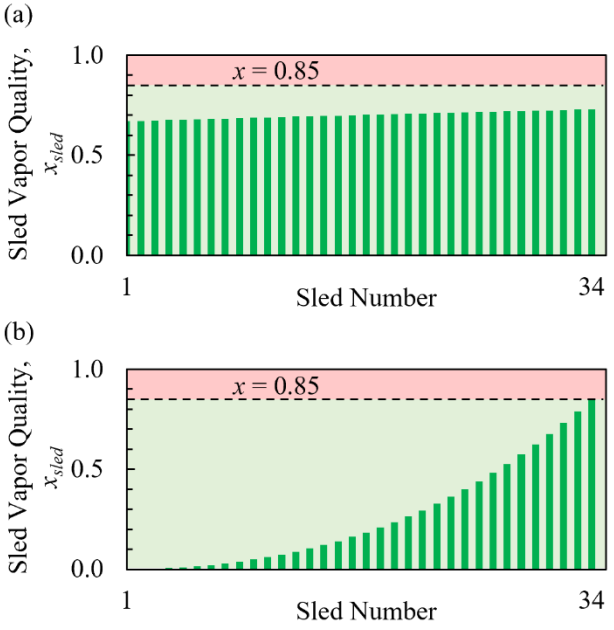

Figure 7. Predicted exit vapor quality distribution under (a) uniform and (b) nonuniform heating with orifice restrictors.

loads from each other. Therefore, the restrictor-free two-phase flow loop is evaluated using a hypothetical heating profile formulated below.

$$Q_{in} = 2\ kW \cdot \left(\frac{y}{H}\right)^2 \qquad [19]$$

where y is the distance from the bottom sled and H is the total height between 34 sleds which are stacked on top of each other. The total heat input under nonuniform heating is 23.01 kW. The sled at the bottom receives no heat whereas the sled at the top receives 2 kW. The heating profile is chosen so that the sleds placed near the top receive higher heat loads. Figure 6.b shows the resulting exit vapor qualities for each sled under nonuniform heating. The exit vapor quality is higher for the sleds near the top. In addition to the gravitational effects, the flow maldistribution is exacerbated by the nonuniform heating. Pressure drop increases with vapor generation, therefore the sleds with higher heat input near the top get lower flow rates. The maximum vapor quality is 1.76, which indicates that the cold plate is under dry-out, and the heat is dissipated through sensible heat of vapor. Dry-out in cold plates results in high thermal resistance that is not acceptable for data center cooling. Without any restrictors, 10 sleds resulted in vapor qualities higher than the 0.85 limit.

An orifice restrictor ($\beta = 2$) is first investigated to suppress maldistribution. The flow resistance factor (α) dictates the resistance to deviations in flow rate. An insufficiently low α value cannot suppress the maldistribution whereas an unnecessarily high value will cause a high pressure drop penalty on the system. Therefore, the orifice needs to be designed precisely for the available flow rate and exit vapor quality requirements. Maldistribution is more severe under nonuniform heating. The value of α is chosen so that the maximum exit vapor quality is 0.85 under the heat load distribution formulated in Equation 19. Figure 7 shows the exit vapor quality distributions under uniform and nonuniform heating for $\alpha = 2.0$. The maximum vapor quality is 0.73 under uniform heating. All the sleds operate under the maximum vapor quality limit. Maldistribution caused by gravitational effects is reduced because the pressure drops across the orifice dominates over the gravitational head. Orifices of varying sizes can be potentially placed in the sleds to cancel out the gravitational head difference along the height, however, this is not investigated in the current study. The maximum vapor quality is 0.85 under nonuniform heating as intended by the orifice design with $\alpha = 2.0$. Therefore, all the sleds operate under the maximum vapor quality limit.

The flow resistance factor (α) is the ratio of orifice to sled pressure drop under maximum heat load without flow maldistribution. For the orifice restrictor ($\beta = 2$), $\alpha = 2.0$ resulted in an acceptable flow distribution and therefore the pressure drop across the orifice needs to be twice as much as the pressure drop across the server sled components. The two-phase flow loop is analyzed for various β values. For each case, α is set to a value that yields a maximum 0.85 vapor quality under nonuniform heating. The resulting α and β pairs can be seen in Figure 8. The value of α, and hence the restrictor pressure drop, decreases with increasing β. The increasingly concave pressure drop-mass flow rate response punishes maldistribution severely meanwhile less pressure drop happens at and below the desired flow rate. The value of α converges to 0 as $\beta \rightarrow \infty$. Therefore, an ideal flow regulator can suppress the maldistribution without causing additional pressure drop to the system at the desired flow rate and maximum heat input.

Lower pressure drop restrictors in a pumped two-phase loop can enable a higher flow rate across the system to dissipate more heat. Therefore, restrictors with higher scaling exponents (β), such as flow regulators, are preferrable. However, there are practical challenges that make their implementation difficult. First, commercially available flow regulators are significantly more costly compared to off-the-shelf orifice restrictors. Second, flow regulators need to be highly tailored for the system which requires a good understanding of the entire

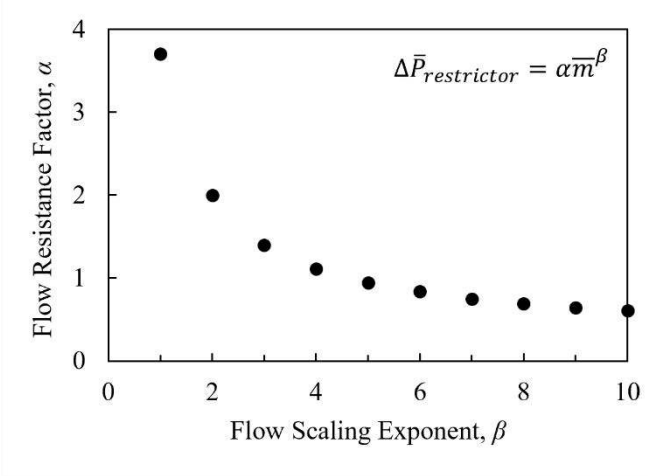

Figure 8. Flow resistance factors needed to obtain a maximum vapor exit quality of 0.85 at various flow scaling exponent values.

pressure drop response of the flow loop under different conditions. If the available flow rate is underestimated, a flow regulator would completely block the additional flow compromising the added cooling capacity. If the available flow is overestimated, a flow regulator would not be effective at suppressing maldistribution. An orifice restrictor is more robust to uncertainty, providing reliable suppression to maldistribution when the system characteristics are not fully characterized.

4. Conclusions

Flow maldistribution due to nonuniform heating is investigated for a two-phase cooling loop for data centers. A numerical model calibrated with experimental results is developed to characterize the flow maldistribution and pressure drop for different heating conditions and flow restrictors. Conclusions are summarized as follows.

- Nonuniform heating in parallel two-phase cooling loops causes flow maldistribution because of the significant pressure drop difference between single-phase cooling and flow boiling. Sleds with higher heat input generate more vapor which increases the pressure drop whereas sleds with lower heat input have less pressure drop. Therefore, the coolant flow rate across increases for the low heat sleds and decreases for the high heat sleds. The maldistribution reduces the maximum heat dissipation from individual sleds under nonuniform heating conditions.
- Flow restrictors can be used to suppress maldistribution at the expense of additional pressure drop to the pumped system. An orifice restrictor, which has quadratic scaling of pressure drop and mass flow rate, requires twice the pressure drop of the server sled to suppress the maldistribution for the investigated system and operating conditions.
- Flow restrictors with higher pressure drop-mass flow rate scaling provide a lower pressure drop penalty. A flow regulator, which provides constant flow rate regardless of the pressure drop, causes no additional pressure drop to the system under the ideal operating conditions. However, there are practical concerns that make their implementation difficult. First, flow regulators are more costly than orifice restrictors. Second, flow regulators require accurate quantification of the system characteristics to be effective unlike orifice restrictors which are reliable under uncertainty.

Acknowledgments

The authors thank Aurelio Munoz for his support in experimental testing.

References

[1] M. A. B. Siddik, A. Shehabi, and L. Marston, "The environmental footprint of data centers in the United States," *Environ. Res. Lett.*, vol. 16, no. 6, p. 064017, Jun. 2021, doi: 10.1088/1748-9326/abfba1.

[2] M. Dayarathna, Y. Wen, and R. Fan, "Data Center Energy Consumption Modeling: A Survey," *IEEE Commun. Surv. Tutor.*, vol. 18, no. 1, pp. 732–794, 2016, doi: 10.1109/COMST.2015.2481183.

[3] F. Rebarber, "Quantifying the Impact on PUE and Energy Consumption When Introducing Liquid Cooling Into an Air-cooled Data Center." Accessed: Jan. 01, 2024. [Online]. Available: https://www.vertiv.com/en-emea/about/news-and-insights/articles/blog-posts/quantifying-data-center-pue-when-introducing-liquid-cooling/#:~:text=Impact%20of%20the%20Introduction%20of,compared%20to%20100%25%20air%20cooling

[4] R. K. Mandel, D. G. Bae, and M. M. Ohadi, "Embedded Two-Phase Cooling of High Flux Electronics Via Press-Fit and Bonded FEEDS Coolers," *J. Electron. Packag.*, vol. 140, no. 3, p. 031003, Sep. 2018, doi: 10.1115/1.4039264.

[5] C. H. Hoang *et al.*, "A Review of Recent Developments in Pumped Two-Phase Cooling Technologies for Electronic Devices," *IEEE Trans. Compon. Packag. Manuf. Technol.*, vol. 11, no. 10, pp. 1565–1582, Oct. 2021, doi: 10.1109/TCPMT.2021.3117572.

[6] W. Chen, T. M. Conboy, G. W. Daines, and D. W. Fogg, "A Robust Two-Phase Pumped Loop with Multiple Evaporators and Multiple Radiators for Spacecraft Applications," presented at the 47th International Conference on Environmental Systems, Charleston, South Carolina, Jul. 2017.

[7] "A, Cicchitti, C. Lombardi, M. Silvestri, G. Soldaini, R. Zavattarelli, 'Two-phase cooling experiments–- pressure drop, heat transfer and burnout measurements,' Energia Nucleare, 7 (1960) 407-425.".

[8] *F. P. Incropera, D. P. DeWitt, T. L. Bergman, A. S. Lavine, "Fundamentals of Heat and Mass Transfer," Wiley, 2011*.

[9] V. Mileikovskyi and T. Tkachenko, "Precise Explicit Approximations of the Colebrook-White Equation for Engineering Systems," in *Proceedings of EcoComfort 2020*, vol. 100, Z. Blikharskyy, Ed., in Lecture Notes in Civil Engineering, vol. 100., Cham: Springer International Publishing, 2021, pp. 303–310. doi: 10.1007/978-3-030-57340-9_37.